Interaction of D-Amino Acid Incorporated Analogues of Pardaxin with Membranes†

Yehonathan Pouny and Yechiel Shai*

Department of Membrane Research and Biophysics, Weizmann Institute of Science, Rehovot, 76100 Israel

Received February 12, 1992; Revised Manuscript Received June 4, 1992

ABSTRACT: The influence of specific L- to D-amino acid substitutions on the interaction of pardaxin, a shark repellent neurotoxin polypeptide, with phospholipid vesicles and human erythrocytes is described. Twelve modified, truncated, or fluorescently labeled [with the fluorophore 7-nitrobenz-2-oxa-1,3-diazole-4-yl (NBD) at their N-terminal amino acid] analogues of pardaxin were synthesized by a solid-phase method. Fluorescence measurements were used to monitor the interaction of the analogues with membranes [Rapaport, D., & Shai, Y. (1991) *J. Biol. Chem. 266*, 23769–23775]. Upon titration of solutions containing the NBD-labeled peptides with small unilamellar vesicles, the fluorescent emission spectra of all NBD-labeled peptides displayed similar blue-shifts, in addition to enhanced intensities, upon relocation of the probe to the more apolar environment. Binding isotherms were constructed from which surface partition constants, in the range of 10^4 M^{-1}, were derived. The existence of an aggregation process, suggested by the shape of the binding isotherms, could be associated only with those analogues in which the N-helix (residues 1–9) was not perturbed. The α-helical content of the analogues was estimated by circular dichroism (CD) spectroscopy, both before and after binding to vesicles at neutral pH. The ability of the peptides to dissipate a diffusion potential and to cause calcein release, as well as to lyse human erythrocytes, served to functionally characterize the peptides. The results support a two α-helix model, with a bend at position 13, as best describing pardaxin in its membrane-bound state. The study also demonstrates that local configurational changes of amino acids, including prolines, do not affect the abilities of the analogues to bind to phospholipid membranes, but do have some effect on their membrane-permeating activities.

The amphipathic α-helix structure is considered to be a common structural feature of most of the peptides capable of forming pores or ion channels. Such structures are found in several putative transmembrane segments of protein channels. One model which attempts to explain the involvement of α-helices in the formation of ion channels suggests that transmembrane amphiphilic α-helices form bundles in which outwardly directed hydrophobic surfaces interact either with other hydrophobic transmembrane segments or with the lipid core of the membrane, while inwardly facing hydrophilic surfaces produce a hollow conducting pore (Inouye, 1974; Guy & Seetharamulu, 1986; Greenblatt et al., 1985). This model is supported by extensive study conducted on the mechanism of action of small pore or ion channel-forming polypeptides. Most of the peptides listed were shown to adopt an amphiphilic α-helical secondary structure in their membrane-bound state. The list includes natural oligopeptides such as the antibiotics alamethicin (Boheim et al., 1983), gramicidin (Fox & Richards, 1982), and cecropins (Christinsen et al., 1988), synthetic putative transmembrane segments of protein channels or designed ion channels (Molle et al., 1988; Oiki et al., 1988a,b; Tosteson et al., 1989; Langosch et al., 1991; Grove et al., 1991; Kennedy et al., 1977; Lear et al., 1988), as well as peptide toxins such as melittin (Tosteson & Tosteson, 1981, 1985; Hanke et al., 1983; Beschiaschvili & Seelig, 1990; Stankowsky et al., 1991) and pardaxin (Moran et al., 1984; Thompson et al., 1986; Shai et al., 1988, 1990).

Pardaxin, a shark repellent neurotoxin, is the major component in the secretion of the Moses Sole flatfish *Pardachirus marmoratus* (Thompson et al., 1986; Shai et al., 1988). Pardaxin, composed of 33 amino acids, possesses a variety of biological activities [reviewed in Lazarovochi et al. (1990)]. At concentrations below 10^{-7} M or at low peptide/lipid molar ratios, pardaxin produces single channels in planar lipid membranes and can induce the selective release of ions but not of calcein from small unilamellar vesicles (Shai et al., 1990, 1991). However, at higher concentrations (10^{-7}–10^{-4} M) cytolysis is induced. The cytolytic activity of pardaxin was shown to be 40–100-fold less than that of the well-characterized hemolytic peptide, the bee venom melittin (Shai et al., 1990). Channels formed by pardaxin are slightly cation-selective and are activated by a transnegative potential. Our recent studies on pardaxin and a series of its synthetic analogues have led to the proposal of a model in which pardaxin, in its membrane-bound state, is composed of two α-helices, both embedded within the lipid bilayer (referred to as either the N- or C-helix, according to the peptide terminal contained within the helix), separated by a proline residue situated at position 13 (Shai et al., 1988, 1990, 1991; Rapaport & Shai, 1991, 1992). Support for this dual α-helix structure was recently provided by NMR studies (Zagorski et al., 1991). The N-terminal α-helix (residues 2–10) is proposed to be involved in the insertion of the peptide into the lipid bilayer and in its subsequent aggregation, while the C-terminal amphiphilic α-helix (residues 13–27) is believed to be part of the putative ion channel-lining segment of pardaxin. The data support a model involving parallel organization of monomers within an aggregate (the "barrel stave" model), as describing the pore formation mechanism of pardaxin and its analogues (Rapaport & Shai, 1991, 1992).

† This research was supported in part by the Israel Cancer Association and by the Basic Research Foundation administered by the Israel Academy of Sciences and Humanities.

* To whom correspondence should be addressed, at the Department of Membranes Research and Biophysics, Weizmann Institute of Science, Rehovot, 76100 Israel. Incumbent of the Adolpho and Evelyn Blum Career Development Chair in Cancer Research.

0006-2960/92/0431-9482$03.00/0

In the present work, we investigate the influence of specific structural distortions within pardaxin, on its ability to interact with and to permeate the membrane. This was achieved by substitution of L-prolines with their D optical isomers, by substitution of two L-leucines with D-leucines (either the pair found side by side within the C-helix or that pair partly in the N- and partly in the C-helix), by synthesizing C-helix-truncated analogues (residues 10–33) in which L-proline at position 13 was substituted either with D-proline or with alanine, or by labeling 33-mer analogues with the fluorophore NBD.[1] The various analogues were investigated in order to characterize the following: (i) secondary structure (using CD spectroscopy); (ii) ability to permeate membranes formed by neutral or acidic phospholipids (either via the induction of dissipation of a diffusion potential or via the release of calcein from small unilamellar vesicles); (iii) binding state and the partition coefficients of fluorescently labeled 33-mer analogues (N^1-NBD-labeled forms) bound to neutral phospholipids; and (iv) cytolytic activity toward human erythrocytes. We present data in support of a two α-helix structure, with a bend at position 13, as describing pardaxin in its membrane-bound state. Moreover, we show that perturbation of the α-helix structure did not affect the abilities of the analogues to bind to membranes; however, it did affect their ability to aggregate there within.

EXPERIMENTAL PROCEDURES

Materials. BOC-Glu(*O*-benzyl)PAM resin and dimethylformamide (peptide synthesis grade) were purchased from Applied Biosystems (Foster City, CA), and BOC amino acids were obtained from Peninsula Laboratories (Belmont, CA). Other reagents for peptide synthesis included trifluoroacetic acid (TFA) (Sigma), *N,N*-(diisopropylethyl)amine (DIEA) (Aldrich; distilled over nonhydrin), dicyclohexylcarbodiimide (DCC) (Fluka), and 1-hydroxybenzotriazole (HOBT) (Pierce). Calcein was purchased from Hach Chemical Co. (Loveland, CO). L-α-Phosphatidylcholine (type IVS) was obtained from Sigma and further purified by the method of Kagawa and Racker (1971). Egg phosphatidylcholine (PC) and phosphatidylserine (PS) from bovine spinal cord (sodium salt, grade I), were purchased from Lipid Products (South Nutfield, U.K.). Cholesterol (extra pure) was supplied by Merck (Darmstadt, Germany) and recrystallized twice from ethanol. 3,3′-Diethylthiodicarbocyanine iodide (diS-C_2-5) was obtained from Molecular Probes (Eugene, OR). NBD-F (4-fluoro-7-nitrobenz-2-oxa-1,3-diazole) was obtained from Sigma. All other reagents were of analytical grade. Buffers were prepared in double glass-distilled water.

Peptide Synthesis and Purification. Peptides were synthesized by the solid-phase method on BOC-Glu(*O*-benzyl)-PAM resin (0.15 mequiv) (Merrifield et al., 1982), as previously described for the synthesis of other pardaxin analogues (Shai et al., 1990). The peptides were cleaved from the resins by HF, extracted with a mixture of acetonitrile/water (1:1 v/v) after HF evaporation, followed by solvent lyophilization. The crude peptide mixtures contained one major peak (as revealed by RP-HPLC) and were shown to be 30–70% pure peptide by weight. The synthesized peptides were purified by RP-HPLC on a C_4 reverse-phase Vydac column (300-Å pore size). The purified peptides were shown to be homogeneous (~99%) by analytical HPLC and subsequent amino acid analysis. The peptides were eluted from the column by a linear gradient of 25–80% acetonitrile in water in the presence of 0.1% TFA for 40 min, at flow rates of 2.5 or 0.9 mL/min, for the semipreparative and analytical columns, respectively.

NBD Labeling of Peptides. Labeling was performed as previously described for pardaxin and its charge-modified analogues (Rapaport & Shai, 1991). Briefly, HPLC-purified peptides (~1–2 mg, TFA salt) were reacted with NBD-F (2 μmol), in dry DMF, for 2–5 h. Product formation was followed by HPLC. Under these conditions, a major product was obtained, possessing an NBD moiety attached to the peptide's N-terminal amino group. The identity of this compound was confirmed by the absence of a dansylated form of the N-terminal glycine residue, after dansylation and subsequent total hydrolysis of the labeled peptide.

Preparation of Liposomes. Small unilamellar vesicles (SUV) were prepared by sonication from soybean lecithin, PC or a PS/PC (1:1 w/w) mixture. Briefly, dry lipid and cholesterol (9:1 w/w) were dissolved in a $CHCl_3$/MeOH mixture (2:1). The solvents were then evaporated under a nitrogen stream, and the lipids (at a concentration of 10 mg/mL) were put under vacuum for 1 h and then resuspended in the appropriate buffer, via vortex mixing (see below). The resultant lipid dispersion was then sonicated for 10–30 min in a bath-type sonicator (G1125SP1 sonicator, Laboratory Supplies Company Inc., New York) until clear. The lipid concentration of the supernatant was determined by phosphorus analysis (Barlett et al., 1959). Vesicles were visualized as follows: A drop containing vesicles was deposited onto a carbon-coated grid and negatively stained with uranyl acetate. The grids were examined using a JEOL JEM 100B electron microscope (Japan Electron Optics Laboratory Co., Tokyo, Japan). Vesicles were shown to be unilamellar with an average diameter of 20–40 nm (Papahadjopoulos & Miller, 1967).

CD Spectroscopy. CD spectra of the peptides were measured with a Jasco J-500A spectropolarimeter under nitrogen after calibrating the instrument with (+)-10-camphorsulfonic acid. The spectra were scanned in a capped quartz optical cell with 0.5-mm path length, at 23 °C. Spectra were obtained for each sample at wavelengths of 250 to 200–190 nm. Three scans were taken at a scan rate of 20 nm/min, with a sampling interval of 0.2 nm. All the peptides were scanned at concentrations of 1.6×10^{-5} M, under three different solvent conditions: (i) in methanol, (ii) in a solution of 50 mM Hepes and 150 mM Na_2SO_4, pH 6.8, and (iii) in solution of 50 mM Hepes and 150 mM Na_2SO_4, pH 6.8, in the presence of vesicles (soybean lecithin). CD spectra were measured at the saturating concentration of the peptides with the lipids [obtained from the maximal change in ellipticity upon titration of the peptides with vesicle solutions (Vogel, 1981; Beschiashvili & Seelig, 1990)].

Fractional helicities (Wu et al., 1981) were calculated as follows:

$$f_h = \frac{([\theta]_{222} - [\theta]^0_{222})}{[\theta]^{100}_{222}} \quad (1)$$

where $[\theta]_{222}$ is the experimentally observed mean residue ellipticity at 222 nm, and values for $[\theta]^0_{222}$ and $[\theta]^{100}_{222}$, corresponding to 0% and 100% helix content at 222 nm, are estimated at 2000 and 30 000 deg·cm²/dmol, respectively (Chen et al., 1974; Wu et al., 1981).

[1] Abbreviations: Pam, (phenylacetamido)methyl; BOC, butyloxycarbonyl; RP-HPLC, reverse-phase high-performance liquid chromatography; DIEA, (diisopropylethyl)amine; HF, hydrogen fluoride; TFA, trifluoroacetic acid; SUV, small unilamellar vesicles; CD, circular dichroism; diS-C_2-5, 3,3′-diethylthiodicarbocyanine iodide; PC, egg phosphatidylcholine; PS, phosphatidylserine; NBD-F, 4-fluoro-7-nitrobenz-2-oxa-1,3-diazole.

Binding Experiments. Binding experiments were conducted as previously described (Rapaport & Shai, 1991). Briefly, SUV (prepared as described above) were added successively to 0.1 μM peptide at 24 °C. Fluorescence intensity was measured as a function of the lipid/peptide molar ratio on a Perkin-Elmer LS-5 Spectrofluorometer, with excitation set at 468 nm, using a 10-nm slit, and emission was set at 530 nm, using a 5-nm slit, in three to four separate experiments. In order to account for the background signal contributed by the lipids to any given signal, the readings observed when unlabeled pardaxin analogues were titrated with lipid vesicles were subtracted from a given recording of fluorescence intensity.

Diffusion Potential Dissipation Experiments; Fluorometric Detection of Membrane Pores. Pore-mediated diffusion potential assays (Sims et al., 1974; Loew et al., 1983, 1985) have been previously described in detail in studies on the permeating properties of pardaxin and some of its analogues (Shai et al., 1990, 1991). In a typical experiment, 4 μL of a liposome suspension, prepared in K^+ buffer (50 mM K_2SO_4, 25 mM Hepes-SO_4^{2-}, pH 6.8), were diluted in 1 mL of isotonic K^+-free buffer (50 mM Na_2SO_4, 25 mM Hepes-SO_4^{2-}, pH 6.8) in a glass tube, to which the fluorescent, potential-sensitive dye diS-C_2-5 (M_r = 492) was then added. A 1-μL sample of a 10^{-7} M valinomycin solution was added to the suspension in order to slowly create a negative diffusion potential inside the vesicles, leading to a quenching of the dye's fluorescence. Once the fluorescence had stabilized, 3–10 min later, pardaxin analogues were added. The subsequent dissipation of the diffusion potential, reflected as an increase in fluorescence, was monitored on a Perkin-Elmer LS-5 Spectrofluorometer, with excitation set at 620 nm and emission at 670 nm, with gain adjusted to 100%. The percentage of fluorescence recovery, F_t, is defined as

$$F_t = [(I_t - I_0)/(I_f - I_0)]100 \quad (2)$$

where I_0 is the initial fluorescence, I_f is the total fluorescence observed before the addition of valinomycin, and I_t is the fluorescence observed after adding the peptide, at time t.

Investigation of Pardaxin Analogue-Induced Calcein Release from Vesicles. Calcein (M_r 623)-containing vesicles [formed from soybean lecithin, PC, or PS/PC (1:1 w/w), all containing 10% (w/w) cholesterol] were prepared with a self-quenching concentration of 60 mM calcein, in 10 mM Hepes, at pH 7.4. The nonencapsulated calcein was removed from the liposome suspension by gel filtration, using a Sephadex G-50 (Pharmacia) column connected to a low-pressure LC system (Pharmacia). In a typical run, 20 μL of the liposome suspension was injected onto the column and eluted in 10 mM Hepes and 150 mM NaCl, pH 7.4. The eluent was monitored by UV spectroscopy (λ = 280 nm), and the vesicles peak was collected and diluted to a volume of 2 mL, in the same buffer. Peptides were added to 1 mL of stirred vesicle suspensions (containing 1.3 μM liposomes). The resulting peptide-induced calcein leakage, reflected as an increase in fluorescence (Allen & Cleland, 1980), was monitored at room temperature on a Perkin-Elmer LS-5 spectrofluorimeter, at an excitation wavelength of 490 nm and an emission wavelength of 520 nm. Complete dye release was obtained after disrupting the vesicles with Triton X-100 (0.1% final concentration). Under experimental conditions, in the absence of peptide, the leakage rate was less than 1% in 5 h. The percentage of fluorescence recovery is defined as described in eq 2; however, here I_f is defined as the total fluorescence observed after addition of Triton X-100.

Table I: Sequences and Designations of Pardaxin Analogues[a]

peptide no.	peptide name[b]	peptide designation
1	D-Pro^7-pardaxin	D-P^7-Par
2	D-Pro^{13}-pardaxin	D-P^{13}-Par
3	D-Leu^5-D-Leu^{19}-pardaxin	D-L^5 L^{19}-Par
4	D-Leu^{18}-D-Leu^{19}-pardaxin	D-L^{18}L^{19}-Par
5	[des 1→9]pardaxin	C-helix
6	D-Pro^{13}-[des 1→9]pardaxin	D-P^{13}-C-helix
7	A^{13}-[des 1→9]pardaxin	A^{13}-C-helix
8	[des 1→9]D-Leu^{19}-pardaxin	D-L^{19}-C-helix
9	[des 1→9]D-Leu^{18}-D-Leu^{19}-pardaxin	D-L^{18}L^{19}-C-helix
10[c]	N^1-NBD-D-Pro^7-pardaxin	NBD-D-P^7-Par
11	N^1-NBD-D-Pro^{13}-pardaxin	NBD-D-P^{13}-Par
12	N^1-NBD-D-Leu^5-D-Leu^{19}-pardaxin	NBD-D-L^{5}L^{19}-Par
13	N^1-NBD-D-Leu^{18}-D-Leu^{19}-pardaxin	NBD-D-L^{18}L^{19}-Par

[a] Substitutions are based on the following sequence of pardaxin: GFFALIPKIISSPLFKTLLSAVGSALSSSGGQE. [b] D denotes the D-configuration of the assigned amino acid. [c] NBD is the abbreviation for 7-nitrobenz-2-oxa-1,3-diazole-4-yl.

Cytolytic Assay. The cytolytic potential of peptides was ascertained as previously described (Weaver et al., 1989; Shai et al., 1990). A 0.5-mL sample of human blood was mixed with 15 mL of PBS, pH 7.3, separated by centrifugation, and washed three times in PBS. The separated red blood cells were diluted 1:1800 with PBS, pH 7.3, and 400 μL of this suspension (~5500 cells/mm^3) were used for light scattering experiments. Light scattering of the suspension was measured both prior to and after the addition of peptide, and the decrease in light scattering was recorded using a Sienco Tm dual sample aggregation meter DP-247E, at 37 °C. At the end of the experiment, Triton X-100 (0.1% final concentration) was added to obtain the maximal decrease of light scattering.

RESULTS

Synthesis of Pardaxin Derivatives. In order to evaluate the contribution of the configuration of specific amino acids within pardaxin to its secondary structure and to its abilities to interact with and to permeate lipid membranes, 12 analogues, truncated forms, or fluorescently labeled analogues of pardaxin were synthesized. Table I lists the peptides and their designations.

Hydrophobic Character of Pardaxin and Its Analogues. In order to determine the relative hydrophobicity of pardaxin and its analogues at neutral conditions, similar to those at which membrane-permeating experiments were performed, pardaxin and its analogues were subjected to reverse-phase HPLC on a C_4 column under neutral conditions (25 mM Na_2HPO_4, pH 7.0), using a linear gradient of 25–80% acetonitrile in water, over a 40-min period. Analysis of the retention times of the various peptide species, summarized in Table II, shows that D-amino acid analogues are consistently retained for shorter times than are the parent peptides, pardaxin and its C-helix, reflecting the more hydrophilic character of the analogues. As the charged amino acids of these peptide species are identical to those of their parent molecules, changes in the hydrophobic character of the analogues would mainly arise from exposure to hydrophilic amino acid residues or amino groups to the surface of the column matrix, due to conformational changes in the secondary structure of the analogues. We can not rule out, however, the contribution of a slight change in the pK of the amino groups due to substitution of a given amino acid.

CD Spectroscopy. The extent of α-helix secondary structures in all the analogues studied was estimated from their

Table II: HPLC Retention Times of Pardaxin and Its Analogues[a]

peptide no.	peptide designation	retention time (min)
1	pardaxin	>60
2	D-P^7-Par	32
3	D-P^{13}-Par	34
4	D-L^5L^{19}-Par	27
5	D-$L^{18}L^{19}$-Par	26
6	C-helix	26
7	D-P^{13}-C-helix	20
8	A^{13}-C-helix	24
9	D-L^{19}-C-helix	18
10	D-$L^{18}L^{19}$-C-helix	17

[a] Elution conditions are as follows: column, C_4 300-Å pore size; solvent A, 25 mM Na_2HPO_4, pH 7.0; solvent B, acetonitrile. A gradient of 25–80% solvent B in A for 40 min, at a flow rate of 0.9 mL/min, was used.

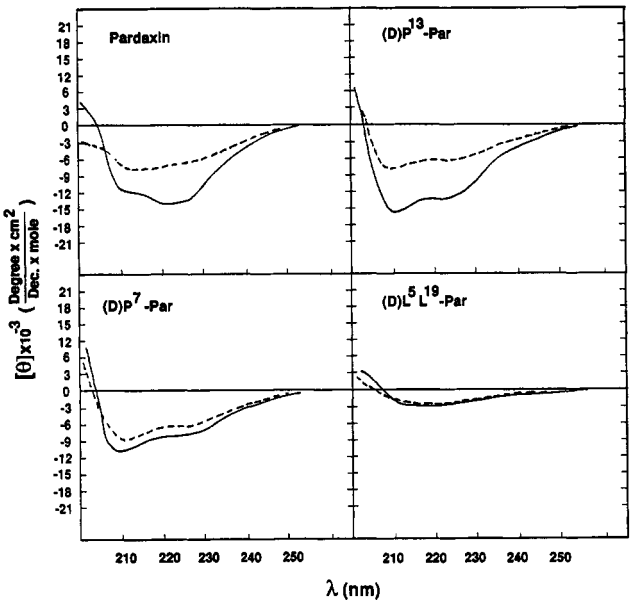

FIGURE 1: CD spectra of pardaxin and some of its analogues in salt solution (dashed lines) and in the presence of soybean lecithin SUV vesicles (continuous line). Spectra were taken as described under Experimental Procedures at a peptide concentration of 1.6×10^{-5} M. Peptide designations are given in the inset.

CD spectra, measured in three solvent systems: (i) in methanol, (ii) in solution (50 mM Hepes, 150 mM Na_2SO_4, pH 6.8), and (iii) in the presence of a saturating concentration of soybean lecithin phospholipid vesicles (pH 6.8). Figure 1 shows the CD spectra of pardaxin, D-P^{13}-Par, D-P^7-Par and D-L^5L^{19}-Par either in solution or in the presence of soybean vesicles.

Table III lists the mean residual ellipticities at 222 nm and the corresponding fractional helicity values (Wu et al., 1981) for pardaxin and its analogues, in the three solvent systems tested. The results can be summarized as follows: (i) The CD spectra of the C-helix and its related analogues, in the three solvent systems tested, are typical of a random coil structure, while slight increases in the α-helical content of a few of the analogues (C-helix, A^{13}-C-helix, and D-P^{13}-C-helix) in the presence of vesicles, as compared to peptides in buffer only, can be observed. (ii) The CD spectra of pardaxin and most of its 33-mer analogues in buffer reflect, for the most part, random coil. However, in the presence of vesicles (in pH 6.8 buffer), the α-helical content of pardaxin and its 33-mer proline-substituted analogues was increased, while that of the other analogues increased only slightly, if at all. Under these conditions, only D-P^{13}-Par has an α-helical content similar to that of pardaxin (24% as compared to 30% in methanol, and 42% as compared to 49% in the presence of vesicles). The order of the α-helical content in the presence of vesicles for the 33-mer analogues is as follows: pardaxin $\approx$ D-P^{13}-Par > D-P^7-Par > D-$L^{18}L^{19}$-Par > D-L^5L^{19}-Par.

Table III: Mean Residual Elipticity $-[\theta]$ at 222 nm and Derived Fractional Helicities of Synthetic Pardaxin and Its Analogues in Methanol, in Solutions of Low Ionic Strength, and in the Presence of Soybean Vesicles

peptide designation[a]	in methanol		in salt (pH 6.8)		in liposomes (pH 6.8)	
	$-[\theta]_{222}$	$[f_h]$	$-[\theta]_{222}$	$[f_h]$	$-[\theta]_{222}$	$[f_h]$
pardaxin[b]	11000	0.30	5800	0.15	15500	0.49
D-P^7-Par	6000	0.13	4540	0.08	9470	0.25
D-P^{13}-Par	9370	0.24	5670	0.12	14660	0.42
D-$F^{15}L^{18}L^{19}$-Par	6610	0.15	5050	0.10	9048	0.25
D-L^5L^{19}-Par	7840	0.19	1300	0	3680	0.06
D-$L^{18}L^{19}$-Par	3820	0.06	2470	0.01	5520	0.12
C-helix[b]	6750	0.16	3800	0.06	6630	0.15
D-P^{13}-C-helix	6300	0.14	1440	0	7550	0.19
A^{13}-C-helix	12500	0.35	3430	0.05	6000	0.13
D-L^{19}-C-helix	0	0	0	0	0	0
D-$L^{18}L^{19}$ C-helix	0	0	0	0	0	0

[a] Peptide designation is according to Table I. [b] Data were taken from Shai et al. (1990).

Fluorescence Studies. The enviromentally sensitive fluorophore NBD has been previously used to describe the environment of the signal peptide of cytochrome *c* oxidase subunit IV (Frey & Tamm, 1990) and of the N- and C-terminals of pardaxin and some of analogues thereof (Rapaport & Shai, 1991). In the present study, the fluorescence emission spectra of the NBD-labeled 33-mer analogues were measured in aqueous solutions or in the presence of vesicles composed of PC at pH 6.8. In these experiments, the lipid/peptide molar ratio was consistently maintained at an elevated level (>3000:1), so that spectral contributions of free peptides could be considered to be negligible. All the peptides exhibited fluorescence emission maxima at 549 nm in buffer and a blue-shift toward 526–528 nm together with a marked increase in their intensities upon the addition of vesicles (pH 6.8). The extent of the blue-shift and the increase in fluorescence intensities were similar to those observed for NBD-pardaxin (Rapaport & Shai, 1991). Therefore, it can be concluded that the N-terminals of the analogues, like that of NBD-pardaxin, are located under the membrane surface (Chattopadhyay & London, 1987).

Characterization of Binding Isotherms and Determination of Partition Constants. The experimental protocols used to obtain the binding isotherms from which surface partition coefficients were calculated have been described in detail elsewhere (Rapaport & Shai, 1991). Generally, peptides at fixed concentrations (0.1 μM) were titrated with PC SUV as described under Experimental Procedures. Observed increases in the fluorescence intensities of the NBD-labeled peptides at pH 6.8 were plotted as a function of the lipid/peptide molar ratios for the different peptides, to give conventional binding curves. An example of such a binding curve is presented in Figure 2 for D-L^5L^{19}-Par. In order to minimize light scattering effects, SUV were used (Mao & Wallace, 1982). The concentrations of the peptides used were low enough such that no disruption of the bilayer structure was assumed. At higher lipid/peptide ratios, we found that the manner in which the lipid component was added, i.e., either as a single dose or in several sequential doses, had no effect on the magnitude of the observed signal.

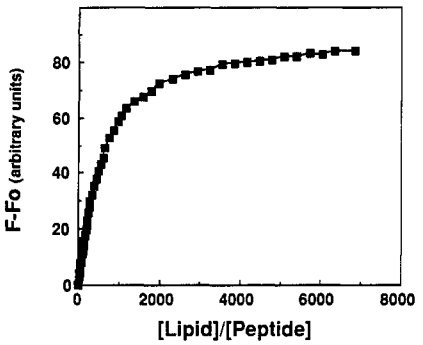

FIGURE 2: Increase in the fluorescence of N^1-NBD-D-L^5L^{19}-Par (0.1 μM total concentration) upon titration with PC vesicles, with excitation at 468 nm and emission monitored at 530 nm. The experiment was performed at 24 °C in 50 mM Na_2SO_4 and 25 mM Hepes-SO_4^{2-}, pH 6.8.

Binding isotherms were analyzed as a partition equilibrium (Rizzo et al., 1987; Schwarz et al., 1986; Beschiaschvili & Seelig, 1990, 1991), using the following formula:

$$X_b = K_p C_f \quad (3)$$

where X_b is defined as the molar ratio of bound peptide per total lipid, K_p corresponds to the partition coefficient, and C_f represents the equilibrium concentration of free peptide in the solution.

In order to calculate X_b, we estimated F_∞, the fluorescence signal obtained when all the peptide is lipid-bound, either from the plateau region of the titration curve or by extrapolation from a double-reciprocal plot of F (total peptide fluorescence) versus C_L (total concentration of lipids), as previously suggested by Schwarz et al. (1986). Knowing the fluorescence intensities of the free and bound forms of the peptide, the fraction of membrane-bound peptide, f_b, could be determined by the formula

$$f_b = (F - F_0)/(F_\infty - F_0) \quad (4)$$

where F represents the fluorescence of peptide after addition of the vesicles and F_0 represents the fluorescence of the unbound peptide. Determining the value of f_b in turn allows us to calculate the equilibrium concentration of free peptide in the solution, C_f, as well as the extent of peptide binding, X_b. Assuming that the peptides bound to the outer half-layer of the SUV (60% of the total lipid), as had been previously suggested (Beschiaschvili & Seelig, 1990), the values of X_b were corrected as such:

$$X_b^* = X_b/0.6 \quad (5)$$

The binding isotherms were obtained by plotting X_b^* versus the concentration of free peptide, C_f, and are presented in Figure 3. Since enough data points of C_f could be collected at very low free peptide concentrations, the surface partition coefficients, K_p, were estimated from the initial slopes of the curves and were found to be $8.6 \pm 1.0 \times 10^4$, $2.1 \pm 0.3 \times 10^4$, $4.6 \pm 0.6 \times 10^4$, and $3.0 \pm 0.3 \times 10^4$ M^{-1} for D-P^{13}-Par, D-P^7-Par, D-$L^{18}L^{19}$-Par, and D-L^5L^{19}-Par, respectively. The estimated K_p values are on the order of 10^4 M^{-1}, similar to those reported for pardaxin (10^4 M^{-1}) (Rapaport & Shai, 1991) and melittin and its derivatives (10^4–10^5 M^{-1}) (Stankowski & Schwarz, 1990), as well as for the staphylococcal δ-toxin (Thiaudière et al., 1991). The binding isotherms for D-P^{13}-Par and D-$L^{18}L^{19}$-Par exhibit a threshold concentration, C_f^*, at which a slight increase in the slope is observed, with D-P^{13}-Par having the largest increase in its slope. However, these C_f^* values correspond to much higher

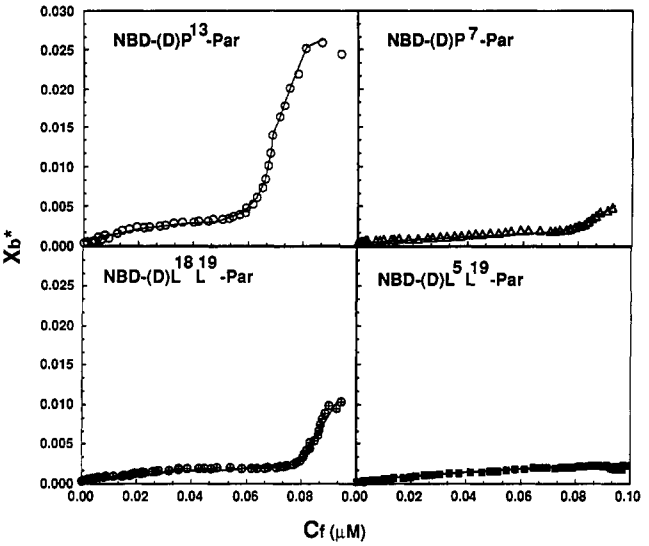

FIGURE 3: Binding isotherms of the NBD-labeled pardaxin analogues, derived from binding curves as shown in Figure 2, by plotting X^*_b (extent of binding) versus C_f (free peptide). Calculations of X^*_b and C_f were performed according to eqs 4 and 5 in the text.

peptide/lipid molar ratios than required for pardaxin, while increases in the slopes are much less sharp than that observed for pardaxin (Rapaport & Shai, 1991). Furthermore, the two analogues reach a plateau at low values of X_b^* (0.01–0.03). The existence of such critical concentrations in the binding isotherms was previously reported for the antibiotic alamethicin (Rizzo et al., 1987) and for pardaxin and a number of its analogues (Rapaport & Shai, 1991). These results were interpreted as reflecting a process whereby peptides first incorporate into the membrane and then aggregate there within (Schwarz et al., 1986, 1987).

Membrane Permeability Evoked by Pardaxin and Its Analogues. (i) *Valinomycin-Mediated Diffusion Potential Assay.* Peptides, at increasing concentrations, were mixed with small unilamellar vesicles (SUV) (at a constant concentration), pretreated with the fluorescent dye diS-C_2-5 and valinomycin. Peptide/lipid molar ratios ranged from 0.0002:1 to 0.1:1. Each experiment was repeated three times with freshly prepared SUV vesicles, with standard deviations calculated to be in the range of 3%. The ability of the peptides to permeate the membrane was elucidated by monitoring the fluorescence recovery until a plateau was observed (usually after 15 min). This level was taken as the maximal activity attainable at each concentration of the tested analogues (see Figure 4A for PC, Figure 4B for PS/PC, and Figure 4C for soybean vesicles). Table IV summarizes the relative potencies of the different peptides as inducers of 20% fluorescence recovery in the three vesicular systems. This level of activity was selected since this represented the maximal value of fluorescence recovery obtained using some of the peptides, even at the highest peptide/lipid ratio tested. The results as presented in Figure 4 and in Table IV can be summarized as follows: (i) Changing the configuration of proline within the N-helix (position 7) results in reduced activity of the analogue D-P^7-Par as compared to that of D-P^{13}-Par or pardaxin, in all vesicle types. (ii) Unlike pardaxin, the activity of the D-proline analogues is dependent on the composition of the lipids, whereas the D-leucine analogues showed a slight dependency on lipid composition. The activity of D-P^{13}-Par was similar to that of pardaxin in the zwitterionic PC vesicles. However, the analogue's activity was about 8–10-fold less in the acidic PS/PC or soybean vesicles (see Table IV). D-P^7-Par was 10–30-fold less potent than pardaxin in all types of vesicles,

Table IV: Peptide/Lipid Molar Ratio Required for Pardaxin and Its Analogues To Induce 20% Fluorescence Recovery[a]

peptide designation	peptide/lipid molar ratio		
	PC	PS/PC	soybean
pardaxin	0.0007	0.0010	0.0010
D-P^{7}-Par	0.0200	0.0070	0.0120
D-P^{13}-Par	0.0010	0.0050	0.0070
D-L^{5}L^{9}-Par	0.0040	0.0065	0.0025
D-L^{18}L^{19}-Par	0.0050	0.0075	0.0025
C-helix	0.100	0.100	0.100
D-P^{13}-C-helix	0.100	>0.100	>0.100
A^{13}-C-helix	>0.100	>0.100	>0.100
D-L^{19}-C-helix	>0.100	>0.100	≫0.10
D-L^{18}L^{19}-C-helix	>0.100	>0.100	≫0.10

[a] Results were determined in a diffusion potential assay in SUV made from three types of lipids: soybean lecithin, PC, and PS/PC(1:1).

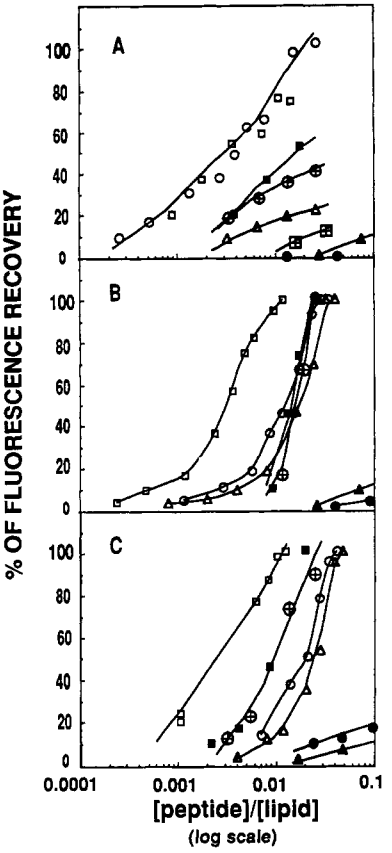

FIGURE 4: Maximal dissipation of the diffusion potential in vesicles by pardaxin and its analogues. Pardaxin in its analogues were added to 1 mL of buffer containing vesicles at a constant concentration (53 μM), preequilibrated with the fluorescent dye diS-C$_2$-5 and valinomycin. Fluorescence recovery, measured after a 15-min interval, is plotted as a function of the peptide/lipid molar ratio. (Trace A) PC vesicles; (trace B) PS/PC (1:1) vesicles; (trace C) soybean lecithin vesicles. Peptide designations are as follows: open squares, pardaxin; open circles, D-P^{13}-Par; open triangles, D-P^{7}-Par; filled triangles, C-helix; crossed squares, A^{13}-C-helix; filled squares, D-L^{5}L^{19}-Par; crossed circles, D-L^{18}L^{19}-Par; filled circles, D-P^{13}-C-helix.

showing the lowest potential of all the long peptide species in the induction of the dissipation of diffusion potentials from PC vesicles. (iii) Some of the truncated peptides were only slightly active (A^{13}-C-helix, D-P^{13}-C-helix), while others (D-L^{19}-C-helix and D-L^{18}L^{19}-C-helix) were not active at all at the maximal peptide/lipid molar ratio tested.

(ii) Calcein Leakage Evoked by Pardaxin and Its Analogues. The potential abilities of pardaxin and its analogues to evoke calcein release from liposomes composed of the phospholipids PC, PS/PC (1:1), or soybean lecithin, at pH 7.4, was examined. Figure 5 shows the dose–response behavior of calcein release induced by the peptides as a function of the peptide/lipid ratio. The results for PC are shown in Figure 5A, for PS/PC in Figure 5B, and for soybean lecithin vesicles in Figure 5C. Table V summarizes the relative potencies of the different peptides as inducers of 20% fluorescence recovery in the three vesicular systems. As in the case of the diffusion potential experiments, this level of activity was selected since this represented the maximal value of calcein release obtained using certain peptides, even at the highest peptide/lipid ratios tested. The time course of fluorescence recovery provides information about the rate of membrane permeation. Figure 6 shows a typical profile of fluorescence recovery as a function of time for the different 33-mer analogues, at concentrations which gave similar activities, using soybean vesicles. Similar profiles were obtained using PC or PS/PC vesicles. Figure

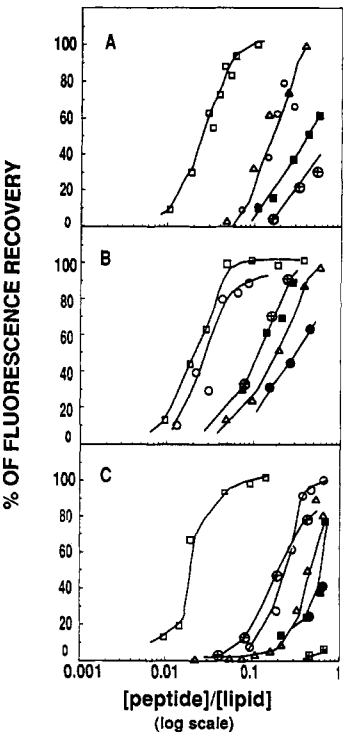

FIGURE 5: Calcein release induced by pardaxin and its analogues as a function of the peptide/lipid molar ratio. Pardaxin or its analogues were added to 1 mL of a 1.7 μM solution of vesicles containing 60 mM calcein, at 25 °C. The leakage of calcein after 10 min was monitored fluorometrically (see Experimental Procedures) and is plotted as a function of the peptide/lipid molar ratio. (Trace A) PC vesicles; (trace B) PS/PC (1:1) vesicles; (trace C) soybean lecithin vesicles. Peptide designations are as in Figure 4.

Table V: Peptide/Lipid Molar Ratio Required for Pardaxin and Its Analogues To Induce 20% Fluorescence Recovery[a]

peptide designation	peptide/lipid molar ratio		
	PC	PS/PC	soybean
pardaxin	0.012	0.015	0.013
D-P^{7}-Par	0.080	0.090	0.300
D-P^{13}-Par	0.030	0.015	0.200
D-L^{5}L^{19}-Par	0.320	0.060	0.400
D-L^{18}L^{19}-Par	0.320	0.060	0.120
C-helix	NA[b]	NA	NA
D-P^{13}-C-helix	NA	0.200	0.300
A^{13}-C-helix	NA	NA	>1.00
D-L^{19}-C-helix	NA	NA	NA
D-L^{18}L^{19}-C-helix	NA	NA	NA

[a] Results were determined in a calcein release assay in SUV made from three types of lipids: soybean lecithin, PC, and PS/PC (1:1). [b] NA, not active at the maximal peptide/lipid molar ratio tested.

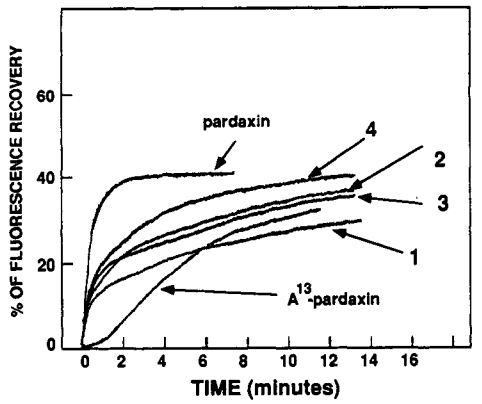

FIGURE 6: Rate of calcein release as a function of time. Pardaxin or its analogues were added to 1 mL of a 1.7 μM solution of vesicles containing 60 mM calcein, at 25 °C. The leakage of calcein was monitored fluorometrically and is plotted as a function of time. The peptides are numbered according to Table I, at the following concentrations: peptide 1, 0.53 μM; peptide 2, 0.3 μM; peptide 3, 0.27 μM; peptide 4, 0.17 μM; pardaxin, 0.05 μM; A13-pardaxin, 0.05 μM.

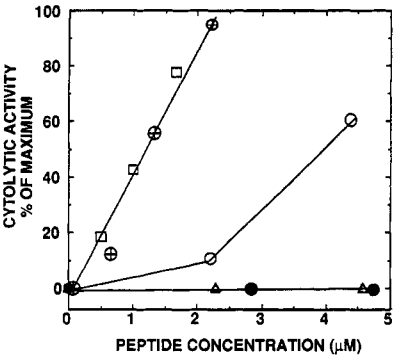

FIGURE 7: Cytolysis of human erythrocytes. Pardaxin or its analogues were added to 400 μL of an erythrocyte suspension (~5500 cells/mm^3 in PBS, pH 7.3, 37 °C), and the percentage of increase in light transmission (decrease in light scattering) was plotted as a function of peptide concentration. Shown is the mean of two experiments, with 5% deviation. Peptide designations are as in Figure 4.

6 also shows the profile of A^{13}-pardaxin for comparison (Shai et al., 1990). The data reveal that all of the 33-mer analogues (i.e., D-P^7-Par, D-P^{13}-Par, D-L^{5}L^{19}-Par, and D-L^{18}L^{19}-Par) could induce leakage of calcein from the vesicles, albeit with different potencies and different rates as compared to pardaxin (at peptide/lipid molar ratios ranging from 0.0025:1 to 0.2:1, the maximum ratio detected). Once again, as shown in the diffusion potential experiments, the activity of the D-amino acids analogues in inducing calcein release from vesicles was dependent on lipid composition, whereas that of pardaxin was not. Moreover, in contrast to the C-helix parent peptide, both truncated analogues A^{13}-C-helix and D-P^{13}-C-helix could induce the release of calcein from the vesicles at high peptide/lipid molar ratio. Thus the order of the activities of the analogues in the different vesicles is as follows: (i) in PC, pardaxin > D-P^{13}-Par > D-P^7-Par > D-L^{5}L^{19}-Par = D-L^{18}L^{19}-Par while all the truncated peptides D-P^{13}-C-helix, A^{13}-C-helix, and C-helix were inactive up to the maximal peptide/lipid molar ration tested. (ii) in PS/PC, pardaxin = D-P^{13}-Par > D-L^{5}L^{19}-Par = D-L^{18}L^{19}-Par > D-P^7-Par > D-P^{13}-C-helix. Both the truncated peptides A^{13}-C-helix and C-helix were inactive up to the maximal peptide/lipid molar ration tested. Finally, (iii) in SB, pardaxin $\gg$ D-L^{18}L^{19}-Par > D-P^{13}-Par > D-P^7-Par $\approx$ D-P^{13}-C-helix $\approx$ D-L^{5}L^{19}-Par > A^{13}-C-helix.

Cytolytic Activity. The cytolytic activity of the peptides was tested by incubation with fresh human erythrocytes and measuring the decrease in light scattering due to erythrocyte lysis, in a 15-min interval. Figure 7 presents the dose–response behavior of peptide-induced lysis of erythrocytes for the various peptide species. The results demonstrate that only pardaxin, D-L^{18}L^{19}-Par, and D-P^{13}-Par were able to lyse the erythrocytes. All the other 33-mer peptide analogues were inactive even at a concentration of 5 μM, the maximal concentration tested. Furthermore, none of C-helix analogues were able to retain the ability of the native sequence to lyse erythrocytes even at concentrations of up to 10 μM, a value 100-fold higher than the minimal concentration at which lysis could be detected with pardaxin (0.1 μM).

DISCUSSION

The presence of an amphiphilic α-helix structure is considered to be an important requirement for membrane-permeating polypeptides. In the present study we have investigated the contribution of the configuration of specific amino acids within pardaxin to its ability to interact with and permeate the membrane. Two major aspects of the various analogues' behavior were studied: First, the structure of the molecules when bound to the membrane was determined, and second, the ability of the analogues to bind to the membrane, to aggregate there within, and ultimately to permeate the membrane were examined. In addition, the ability of the analogues to lyse human erythrocytes was also tested.

The Structure of Pardaxin within the Membrane. Changing the configuration of the proline residue located at position 13 yielded an analogue maintaining most of the properties of pardaxin. This was verified by three criteria: (i) the modified peptide has CD spectra similar to that of pardaxin, (ii) the analogue is as active as pardaxin in inducing the dissipation of diffusion potential from PC vesicles, and in the release of calcein from PS/PC vesicles, and (iii) compared to the other analogues tested, it most readily aggregates within the membrane (as indicated by the shape of its binding isotherm). These results support our model whereby Pro^{13}, in contrast to Pro^7, does not participate in the formation of an α-helix but rather serves as a hinge between the N-helix and the C-helix. Further support for the presence of a hinge between the two helices comes from studies showing that substitution of the proline residue found at position 13 with alanine, an α-helix former, resulted in the formation of an analogue, A^{13}-Par, with a substantially increased α-helical content (100% α-helix) (Shai et al., 1990); this was later confirmed by the determination of pardaxin structure in solution, by NMR (Zagurski et al., 1991).

A common feature of D-P^7-Par and D-L^{5}L^{19}-Par is that both display penetration of disordered N-terminal segments into the membrane, as revealed by the blue-shift of their emission spectra in the presence of vesicles. Moreover, both were unable to form large aggregates within the membrane, as observed by the shapes of their binding isotherms. This might suggest that, in the N-terminal segment of pardaxin, an α-helix structure is necessary for aggregation within the membrane to occur. In this light, the observed ability of these analogues to induce calcein release from SUV at very high peptide/lipid molar ratios might result from the formation of defects in the membrane itself rather than from the formation of large pores.

The Role of Proline in Membrane Permeation. It has been suggested that the relative abundance of proline residues in the putative transmembrane helices of membrane transport proteins may reflect their importance for membrane insertion

or for the actual transport process (Brandl & Deber, 1986; Barlow & Thornton, 1988; Deber et al., 1990). Partial support for such a claim comes from several studies involving proteins in which the proline residues found within their putative transmembrane segments had been mutated. Such proteins include bacteriorhodopsin (Mogi et al., 1989), Ca^{2+} ATPase (Vilsen et al., 1989), and the lac permease (Lolkema et al., 1988; Consler et al., 1991). Proline is an *imino* acid incapable of participating in hydrogen bonding and thus may introduce structural distortion, in the form of a bend, into the transmembrane helix. This proposed bend may allow for the formation of a "funnel"-shaped pore by the segments/peptides, in which proline residues, situated on the convex side of the helix, point toward the hydrated center of the pore. Such a structure was suggested for the conformation assumed by alamethicin within the membrane (Fox & Richards, 1982) as well as for melittin (Terwilliger et al., 1982). Such a structure may also be realized by pardaxin. The data in the present study reveal that neither the configuration nor in fact the presence of proline is essential for the membrane-binding and permeating properties of pardaxin, since all the 33-mer analogues have approximately the same partition coefficient as pardaxin. All these analogues, including A^{13}-Par (Shai et al., 1990), could permeate the membrane, albeit at different potencies and rates.

The bee venom melittin and the antibacterial cecropines are membrane-permeating polypeptides that have also been shown to form voltage-activated ion channels. When proline residues were substituted by alanine in melittin (Dempsey et al., 1991) or by glutamic acid in cecropines (Christensen et al., 1988), part of the permeating activity of the parent molecules was preserved in the analogues. However, voltage activation of the channels, as induced by the analogues, was abolished, probably due to the absence of the hinge region formed by the presence of proline residues. It also has been proposed that a mechanism of ion channel operation may include cis/trans isomerization of proline residues occurring simultaneously with ion transfer (Brandl & Deber, 1986; Deber et al., 1990). Although a major difference exists between cis/trans conformational changes and L to D configurational changes, in both cases, in functional terms, only the orientation of the N-helix to the C-helix of pardaxin is affected. Single-channel measurements are currently in progress aimed at determining the properties of the channels formed by D-amino acid analogues of pardaxin.

One interesting result of the current study is that the D-amino acid analogues displayed different permeating potentials in vesicles composed of a variety of phospholipids. For instance, the permeating activity of D-P^{13}-Par varied up to 10-fold, depending upon the charge of the phospholipid head group. This property might result from the exposure of charges or of hydrophilic amino acid residues within the peptides to the vesicle surface, due to conformational changes within the peptides' backbones caused by the L to D configurational substitutions (as revealed by the change in HPLC retention times). Moreover, both A^{13}-C-helix and D-P^{13}-C-helix could induce calcein release from acidic vesicles, a property not realized by the C-helix or its D-Leu analogues.

Finally, the ability of D-P^{13}-Par and D-$L^{18}L^{19}$-Par, but not of D-P^{7}-Par or D-$L^{5}L^{19}$-Par, to lyse human erythrocytes correlates with the ability of the former pair to form aggregates within the membrane (as revealed by the shape of their binding isotherms), a property previously observed for pardaxin and some of its analogues (Shai et al., 1991). Both the decreases in the lytic activity as well as the difference in the potencies of the various D-amino acid analogues to permeate membranes composed of different phospholipids raises the possibility for local D-amino acid substitution in antimicrobial-active polypeptides as a means of reducing their lytic activities. The antimicrobial activities of polypeptides such as cecropines, magainin (Zasloff, 1987), or melittin are believed to result from membrane perturbation rather than from specific recognition patterns, since fully substituted D-amino acid analogues of cecropines and maginin have been recently shown to possess the same activity as their parent molecules (Wade et al., 1990; Bessalle et al., 1990). It should be noted, however, that the cytolytic activity of pardaxin is 40–100-fold less than that of melittin (Shai et al., 1990). Melittin is believed to adsorb mainly onto the surface of the membrane, while pardaxin was shown to aggregate within the membrane. Therefore, the mechanism of their cytolysis is probably different.

In summary, the results support a two α-helix model, with a bend at position 13, as best describing pardaxin in its membrane-bound state. In this model, an ordered α-helical structure is presumably required for the hydrophobic N-terminal segment, found within the lipidic bilayer core, for efficient aggregation within the membrane, and for the formation of large pores, at relatively low peptide/lipid molar ratios. This study also demonstrates that local configurational changes of amino acids, including prolines, do no affect the abilities of the various analogues to bind to phospholipid membranes. Our data do not, however, allow us to rule out the influence of such changes on the ion-channel properties of pardaxin. Work in our laboratory is currently addressing this question.

ACKNOWLEDGMENT

We thank Aurelia Finkels for her technical assistance.

REFERENCES

Allen, T. M., & Cleland, L. G. (1980) *Biochim. Biophys. Acta 597*, 418–426.
Barlett, G. R. (1959) *J. Biol. Chem. 234*, 466–468.
Barlow, D. J., & Thornton, J. M. (1988) *J. Mol. Biol. 201*, 601–619.
Beschiaschvili, G., & Seelig, J. (1990) *Biochemistry 29*, 52–58.
Bessalle, R., Kapitkovsky, A., Gorea, A., Shalit, I., & Fridkin, M. (1990) *FEBS Lett. 274*, 151–155.
Boheim, G., Hanke, W., & Yung, G. (1983) *Biophys. Struct. Mech. 9*, 181–191.
Brandl, C. J., & Deber, C. M. (1986) *Proc. Natl. Acad. Sci. U.S.A. 83*, 917–921.
Chattopadhyay, A., & London, E. (1987) *Biochemistry 26*, 39–45.
Chen, Y. H., Yang, J. T., & Chau, K. H. (1974) *Biochemistry 13*, 3350–3359.
Christensen, B., Fink, J., Merrifield, R. B., & Mauzerel, D. (1988) *Proc. Natl. Acad. Sci. U.S.A. 85*, 5072–5076.
Consler, T. G., Orestes, T., & Kaback, H. R. (1991) *Biochemistry 30*, 1291–1298.
Deber, C. M., Sorrell, B. J., & Xu, G. Y. (1990) *Biochem. Biophys. Res. Commun. 172*, 862–869.
Dempsey, C. E., Bazzo, R., Harvey, T. S., Syperek, I., Boheim, G., & Campbell, I. D. (1991) *FEBS Lett. 281*, 240–244.
Fox, R. O., & Richards, F. M. (1982) *Nature 300*, 325–330.
Frey, S., & Tamm, L. K. (1990) *Biochem. J. 272*, 713–719.
Greenblatt, R. A., Blatt, Y., & Montal, M. (1985) *FEBS Lett. 193*, 125–134.
Grove, A., Tomich, J. M., & Montal, M. (1991) *Proc. Natl. Acad. Sci. U.S.A. 88*, 6418–6422.

Guy, H. R., & Seetharamulu, P. (1986) *Proc. Natl. Acad. Sci. U.S.A. 83*, 508–512.
Hanke, W., Methfessel, C., Wilmsen, H. U., Katz, E., Jung, G., & Boheim, G. (1983) *Biochim. Biophys. Acta 727*, 108–114.
Inouye, M. (1974) *Proc. Natl. Acad. Sci. U.S.A. 71*, 2396–2400.
Kagawa, Y., & Racker, E. (1971) *J. Biol. Chem. 246*, 5477–5487.
Kennedy, S. J., Roeske, R. W., Freeman, A. R., Watanabe, A. M., & Besch, H. R., Jr. (1977) *Science 196*, 1341–1342.
Langosch, D., Hartung, H., Grell, E., Bamberg, E., & Betz, H. (1991) *Biochim. Biophys. Acta* 1063, 36–44.
Lazarovici, P., Primor, N., Genaro, J., Fox, J., Shai, Y., Lelkes, P. I., Caratsch, C. G., Raphunathan, G., Guy, H. R., Shih, Y. L., & Edwards, C. (1990) in *Marine Toxins: Origins, Structure and Pharmacology* (Holl, S., & Strichartz, J., Eds.) ACS Series 418, pp 347–364, Washington, DC.
Lear, J. D., Wasserman, Z. R., & DeGrado, W. F. (1988) *Science 240*, 1177–1181.
Loew, L. M., Rosenberg, I., Bridge, M., & Gitler, C. (1983) *Biochemistry 22*, 837–844.
Loew, L. M., Benson, L., Lazarovici, P., & Rosenberg, I. (1985) *Biochemistry 24*, 2101–2104.
Lolkema, J. S., Püttner, I. B., & Kaback, H. R. (1988) *Biochemistry 27*, 8307–8310.
Mao, D., & Wallace, B. A. (1984) *Biochemistry 23*, 2667–2673.
Merrifield, R. B., Vizioli, L. D., & Boman, H. G. (1982) *Biochemistry 21*, 5020–5031.
Mogi, T., Stern, L. J., Chao, B. H., & Khorana, H. G. (1989) *J. Biol. Chem. 264*, 14192–14196.
Molle, G., Dugast, J. Y., Ducloheir, H., Daumas, P., Heitz, F., & Spach, G. (1988) *Biophys. J. 53*, 193–203.
Moran, A., Korchak, Z., Moran, N., & Primor, N. (1984) in *Toxins, Drugs and Pollutants in Marine Animals* (Bolis, L., Zadunaisky, J., & Gilles, R., Eds.) pp 13–25, Springer Verlag, Berlin.
Oiki, S., Danho, W., & Montal, M. (1988a) *Proc. Natl. Acad. Sci. U.S.A. 85*, 2393–2397.
Oiki, S., Danho, W., Madison, V., & Montal, M. (1988b) *Proc. Natl. Acad. Sci. U.S.A. 85*, 8703–8707.
Papahadjopoulos, D., & Miller, N. (1967) *Biochim. Biophys. Acta 135*, 624–638.
Rapaport, D., & Shai, Y. (1991) *J. Biol. Chem. 266*, 23769–23775.
Rapaport, D., & Shai, Y. (1992) *J. Biol. Chem. 267*, 6502–6509.
Rizzo, V., Stankowsky, S., & Schwarz, G. (1987) *Biochemistry 26*, 2751–2759.
Schwarz, G., Stankowsky, S., & Rizzo, V. (1986) *Biochim. Biophys. Acta 861*, 141–151.
Schwarz, G., Gerke, H., Rizzo, V., & Stankowsky, S. (1987) *Biophys. J. 52*, 685–692.
Shai, Y., Fox, J., Caratsch, C., Shih, Y. L., Edwards, C., & Lazarovici, P. (1988) *FEBS Lett. 242*, 161–166.
Shai, Y., Bach, D., & Yanovsky, A. (1990) *J. Biol. Chem. 265*, 20202–20209.
Shai, Y., Hadari, Y. R., & Finkels, A. (1991) *J. Biol. Chem. 266*, 22346–22354.
Sims, P. J., Waggoner, A. S., Wang, C. H., & Hoffmann, J. R. (1974) *Biochemistry 13*, 3315.
Stankowsky, S., & Schwarz, G. (1990) *Biochim. Biophys. Acta 1025*, 164–172.
Stankowsky, S., Pawlak, M., Kaisheva, E., Robert, C. H., & Schwarz, G. (1991) *Biochim. Biophys. Acta 1069*, 77–86.
Thiaudière, E., Siffert, O., Talbot, J. C., Bolard, J., Alouf, J. E., & Dufourcq, J. (1991) *Eur. J. Biochem. 195*, 203–213.
Thompson, S. A., Tachibana, K., Nakanishi, K., & Kubota, I. (1986) *Science 233*, 341–343.
Tosteson, M. T., & Tosteson, D. C. (1981) *Biophys. J. 36*, 109–116.
Tosteson, M. T., Alvarez, O., & Tosteson, D. C. (1985) *Regul. Pept. (Suppl. 4)*, 39–46.
Tosteson, M. T., Auld, D. S., & Tosteson, D. C. (1989) *Proc. Natl. Acad. Sci. U.S.A. 86*, 707–710.
Terwilliger, T. C., Weissman, L., & Eisenberg, D., (1982) *Biophys. J. 37*, 353–361.
Vilsen, B., Andersen, J. P., Clarke, D. M., & Maclennan, D. H. (1989) *J. Biol. Chem. 264*, 21024–21030.
Vogel, H. (1981) *FEBS Lett. 134*, 37–42.
Weaver, A., Kemple, M. D., & Prendergast, F. G. (1989) *Biochemistry 28*, 8624–8639.
Wade, D., Boman, A., Wahlin, B., Drain, C. M., Andreu, D., Boman, H. G., & Merrifield, R. B. (1990) *Proc. Natl. Acad. Sci. U.S.A. 87*, 4761–4765.
Woolfson, D. N., & Williams, D. H. (1990) *FEBS Lett. 277*, 185–188.
Woolfson, D. N., Mortishire-Smith, R. J., & Williams, D. H. (1991) *Biochem. Biophys. Res. Commun. 175*, 733–737.
Wu, C. S. C., Ikeda, K., & Yang, J. T. (1981) *Biochemistry 20*, 566–570.
Zagorski, M. G., Norman, D. G., Barrow, C. J., Iwashita, T., Tachibana, K., & Patel, D. J. (1991) *Biochemistry 30*, 8009–8017.
Zasloff, M. (1987) *Proc. Natl. Acad. Sci. U.S.A. 84*, 5449–5453.